Journal of Nuclear Materials 398 (2010) 93–99

Contents lists available at ScienceDirect

Journal of Nuclear Materials

journal homepage: www.elsevier.com/locate/jnucmat

Study on low activation decoupler material for MW-class spallation neutron sources

M. Harada *, M. Teshigawara, F. Maekawa, M. Futakawa

Materials and Life Science Division, J-PARC Center, Japan Atomic Energy Agency, Tokai-mura, Naka-gun, Ibaraki-ken 319-1195, Japan

A B S T R A C T

The Japan Spallation Neutron Source (JSNS) at the Japan Proton Accelerator Research Complex (J-PARC) has started its operation on May 30, 2008. The Ag–In–Cd (AIC) alloy was adopted as a decoupler material for two decoupled moderators. A high decoupling energy at 1 eV was for the first time achieved in MW-class spallation neutron sources due to the adoption of the AIC alloy. Although the AIC decoupler is superior in the neutronic performance, it has a demerit in high residual radioactivity due to production of Ag-110 m (half life: 250 days) and Ag-108 m (half life: 418 years). To overcome this demerit, we studied on possibilities of a low activation decoupler material with high decoupling energy as the AIC alloy, that is, Au–In–Cd (AuIC) alloy. Neutronic performance of this material was investigated by using neutronics calculations. As a result, it was found that the AuIC decoupler could provide neutron pulses with almost the same characteristics as those for the AIC decoupler even when the burn-up effects were considered. Excellent low activation property of the AuIC alloy to the AIC alloy was demonstrated by residual radioactivity calculations. On viewpoint of neutronics performance, it was concluded that the AuIC decoupler was available as the substitute of the AIC decoupler.

1. Introduction

The Japan Spallation Neutron Source (JSNS) at the Japan Proton Accelerator Research Complex (J-PARC) produced the first neutrons on May 30, 2008. As shown in Fig. 1, a Mercury (Hg) target, a Beryllium (Be)–Iron (Fe) combined type of reflector and three supercritical Hydrogen (H_2) moderators compose the central part of the JSNS. The three moderators in JSNS are coupled one (CM) to provide a high intensity pulse, unpoisoned decoupled one (DM) and poisoned decoupled one (PM) to provide a narrow pulse with a short tail. Fig. 2 shows a detailed figure of DM of the JSNS. For DM and PM, a decoupler, thermal neutron absorber, is located around the moderator to eliminate slow neutrons into the moderator. A decoupling energy (E_d), which is the energy to be $1/e$ neutron transmission, is index of performance of a decoupler. A decoupled moderator with higher E_d provides a shorter tail pulse with a certain intensity penalty.

For high resolution experiments in the JSNS, the decoupled moderators with higher E_d are desirable. Until recently, a candidate of decoupler material to realize $E_d \sim 1$ eV was only boron (B) provided by boron carbide (B_4C). However, in the intense neutron source, the large helium (He) gas production rate due to the $^{10}B(n, \alpha)$ reaction leads to serious problems (swelling). In addition, E_d of B_4C changes according to a burn-up of B. Therefore, such a candidate is limited to a decoupler material based on the (n, γ) reaction. The E_d for cadmium (Cd) decoupler that is often used for intense spallation neutron sources is only 0.3 eV. In order to realize $E_d = 1$ eV, we considered to combine thermal neutron absorber and neutron absorbers with resonance absorption. As such the decoupler material, we proposed silver–indium–cadmium (Ag–In–Cd, AIC) alloy used as a control rod in the Pressured Water Reactor [1]. Fig. 3 shows transmissions of the AIC decoupler and the B_4C one as a function of neutron energy, E_n. This B_4C decoupler is controlled by density of ^{10}B to be $E_d = 1$ eV. The curve of the AIC is fluctuating around the B_4C curve, which is proportional to $1/\sqrt{E}$ and E_d of the AIC seems to be about 1 eV. By optimizing the thickness and the composition of the AIC decoupler from results of neutronics calculations, excellent pulse shape can be sustained until the assumed life time of 30,000 h in 1 MW operation (30,000 MWh as a time-integrated proton beam power). At the same time, it is satisfied that the AIC alloy stays in a single phase until the assumed life time to keep material properties stable. Via not only such the optimization study, but also the manufacturing feasibility test and the bonding test with aluminum alloy, $E_d = 1$ eV has been realized for the two decoupled moderators of JSNS for the first time in MW-class spallation neutron sources by the adoption of AIC decoupler [2,3].

The AIC alloy has a significant demerit of high residual radioactivity due to production of ^{110m}Ag (half life ($T_{1/2}$): 250 days) and ^{108m}Ag ($T_{1/2}$: 418 years). This demerit makes handling and storages of used moderators difficult. Of course, this is taken into account in the design of JSNS. However, recently, this is closed up on viewpoint of an improvement of the storage scenario and a promotion

* Corresponding author. Tel.: +81 29 282 6217; fax: +81 29 282 6496.
E-mail address: harada.masahide@jaea.go.jp (M. Harada).

0022-3115/$ - see front matter © 2009 Elsevier B.V. All rights reserved.
doi:10.1016/j.jnucmat.2009.10.016

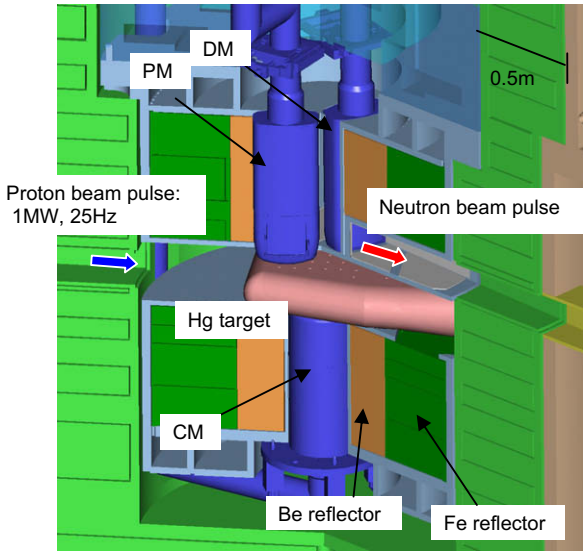

Fig. 1. Schematic view of Target–Moderator–Reflector assembly in JSNS.

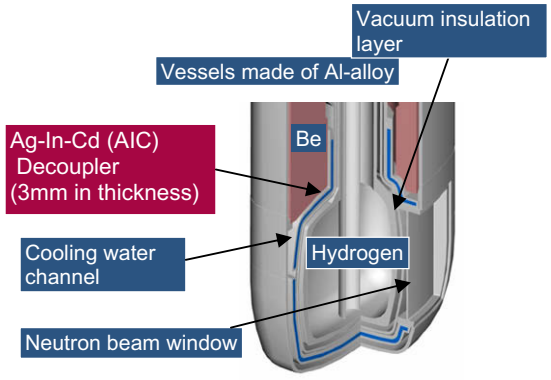

Fig. 2. Schematic view of DM.

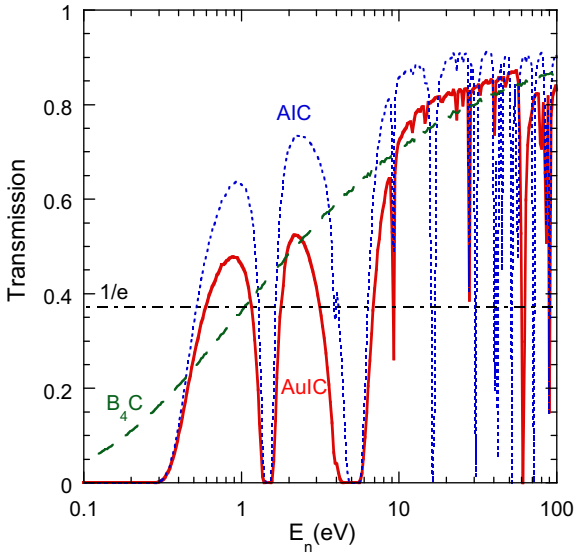

Fig. 3. Neutron transmission of AuIC, AIC and B_4C (E_d = 1 eV).

of the environmental preservation. Therefore, development of a new decoupler material with keeping high E_d and good material property like the AIC decoupler is indispensable. As alternative decoupler materials, B based one and Cd one are generally considered. The both decouplers have low residual radioactivity. However, as already mentioned, the B based decoupler has the burn-up problem and E_d = 1 eV cannot be achieved by the Cd decoupler. To overcome this situation, we propose a new decoupler material, gold–indium–cadmium (Au–In–Cd, AuIC) alloy, as a composite decoupler. Ag in the AIC alloy that is the origin of high radioactivity is replaced with Au in the AuIC alloy. Note that Au and Ag are in the same group in the periodic table, and Au can solve In and Cd like Ag. It is an advantage as a decoupler material that Au itself is a neutron absorber. As shown in Fig. 3, the transmission curve of the AuIC is similar to that of the AIC and E_d of the AuIC also seems to be about 1 eV. As the first stage, by a comparison with the AIC decoupler on viewpoint of neutronics, it needs to clarify whether the AuIC decoupler can be used as the substitute of the AIC decoupler or not.

In this paper, we studied the AuIC decoupler by neutronics calculation on viewpoint of pulse characteristics, residual radioactivity and burn-up effect. By comparison with the AIC decoupler, we discussed about feasibility of the AuIC decoupler.

2. Calculation model and method

A simple calculation model of JSNS was used in the neutronics calculation. In this model, a rectangular parallelepiped Hg target, a rectangular parallelepiped H_2 moderator, the Be–Fe reflectors with neutron beam hole and the decoupler were taken into account. Any containers were not equipped with in these components. An incident proton beam into the target is 3 GeV and 1 MW with the repetition rate of 25 Hz. Major parameters in the simple calculation model summary in Table 1. Fig. 4 shows vertical cross sectional view of the simple calculation model at the moderator center.

For the neutronics calculation, the PHITS code [4] and the MCNP code [5] with JENDL evaluated cross section library [6,7] were used. These codes simulate proton and neutron transports in the all energy region and provide neutron flux spectra. For the pulse characteristics calculation, a point estimator at 10 m from the moderator surface was used.

For the calculation of the residual radioactivity, the DCHAIN-SP code [8] was used. For this calculation, the proton beam power of 1 MW and the operation time of 6 years (5000 h per year) were assumed. Irradiation pattern per one year is combination of a 5000 h operation and a 3760 h cooling after it. The time-integrated proton beam power is indicated as (P_i), and P_i = 30,000 MWh corresponds to the assumed life time of the moderator.

Table 1
Major parameters for simple calculation model.

Target	Material	Hg
	Shape	Rectangular parallelepiped
	Size	$40^{W} \times 8^{H} \times 60^{L}$ cm^3
Moderator	Material	Super-critical H_2
	Temperature	20 K
	Pressure	1.5 MPa
	Shape	Rectangular parallelepiped
	Size	$12^{W} \times 12^{H} \times 5^{T}$ cm^3
	Position	Below the target
Decoupler	Material	AuIC
	Thickness	3 mm
Reflector	Material	Inner: Be
		Outer: Fe
	Shape	Cylindrical
	Size	Inner: $60^{\varphi} \times 60^{H}$ cm^3
		Outer: $120^{\varphi} \times 120^{H}$ cm^3
Neutron beam line	Size	10×10 cm^2
	Opening angle	25° on both sides

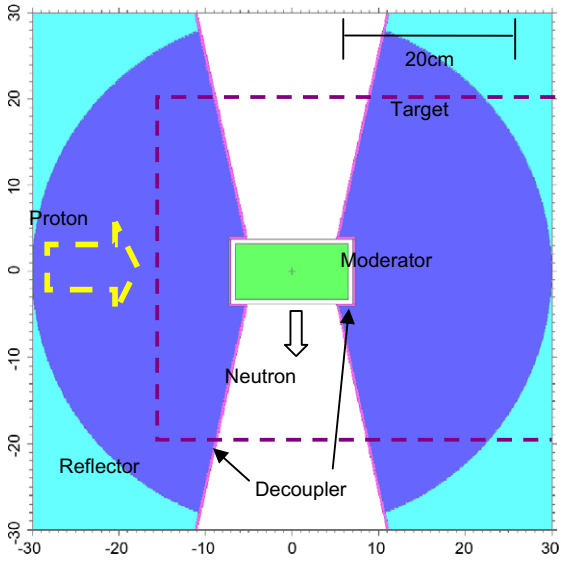

Fig. 4. Vertical cross sectional view of simple calculation model. Positions of target and proton are really upper plane (not the same plane depicted).

For the burn-up calculation, the decoupler cell in the simple model was divided into 10 sections according to neutron flux intensity to consider difference of the intensity. Moreover, the decoupler thickness of 3 mm was also divided into six layers. By the burn-up calculation in these divided cells, the burn-up effect could be precisely represented. The following most important reactions were considered as burn-up reactions.

^{115}In(n,γ) ^{116}In ($T_{1/2}$: 54 m) ≫ ^{116}Sn (Stable)
^{113}Cd(n,γ) ^{114}Cd (Stable)
^{197}Au(n,γ) ^{198}Au ($T_{1/2}$: 2.8 d) ≫ ^{198}Hg (Stable)

The reason to choose these reactions is that changes of amounts of parent nuclei in these reactions have an effect on pulse characteristics due to their neutron absorption cross sections much larger than other reactions. In the burn-up calculation, neutron fluxes and reaction rates in every cell are calculated every time step. The amounts of the changed isotopes are obtained from these data and reflect to the calculation in the next time step. These calculations are iterated during the operation from the start to the end. Time step in this calculation is 5000 MWh. Pulse calculation is also done at every time step.

3. Results and discussions

3.1. Burn-up effect on pulse characteristics

Composition of the AuIC alloy was determined with two criteria. The first one was that pulse shapes did not deteriorate by the burn-up effects throughout the life time of the decoupler. The second one was that the alloy stayed in a single phase (Au solution) when the alloy was burned until the life time. The reason to stay the single phase is that stability of material property is expected. The optimum initial composition was finally found as shown in Table 2 after many try and error calculations. The composition at P_i = 30,000 MWh is also shown in Table 2. By the burn-up of Au and In, Hg of 5.3% and Tin (Sn) of 0.16%, respectively, are produced at the life time.

Fig. 5 shows composition of the burning isotopes (^{113}Cd, ^{115}In and ^{197}Au) as a function of P_i at a position of the highest neutron flux averaged over the thickness direction. Reduction of ^{113}Cd is

Table 2
Composition of AuIC decoupler at P_i = 0 and 30,000 MWh.

P_i (MWh)	0	30,000
Material	Composition (%)	
Au	75.6	70.3
Cd	25	25
In	0.4	0.24
Hg	–	5.3
Sn	–	0.16

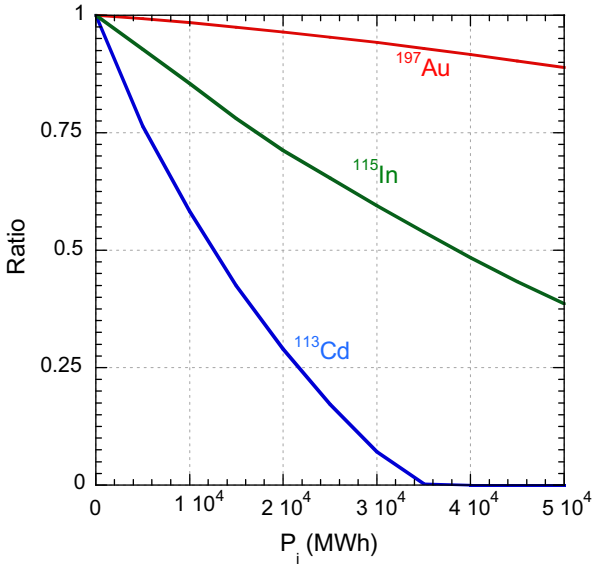

Fig. 5. Composition of isotopes in AuIC decoupler as a function of P_i amount of each isotope is normalized to be 1.0 at the beginning of the operation.

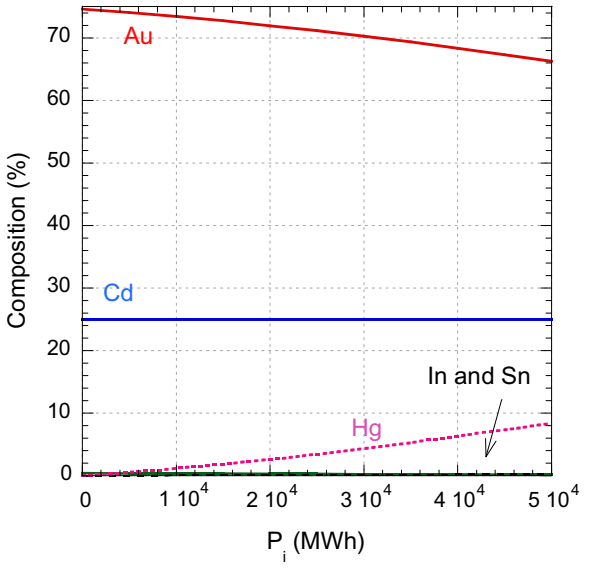

Fig. 6. Composition of each element in AuIC decoupler as a function of P_i.

the fastest among the three neutron absorbing isotopes. The ^{113}Cd nuclei almost disappear at P_i = 35,000 MWh. Fig. 6 shows composition of each element in the AuIC as a function of P_i at a position of the highest neutron flux averaged over the thickness direction. Changes of In and Sn are negligible during the operation. Although ^{113}Cd reduced the fastest as shown in Fig. 5, change of

^{113}Cd is also negligible. The reason is that ^{113}Cd is changed to only the same element, ^{114}Cd, by the burn-up. Au is slowly changed to Hg due to the burn-up of ^{197}Au. Fig. 7 shows pulse shapes at E_n = 2 and 50 meV with several P_i. Although pulse shapes do not change up to P_i = 30,000 MWh, they deteriorate significantly after $P_i \geqslant$ 40,000 MWh, especially in their tail portion. Fig. 8 shows binary phase diagrams of Au–Cd, Au–In, Au–Hg and Au–Sn systems [9]. Vertical thick broken lines indicate the composition at

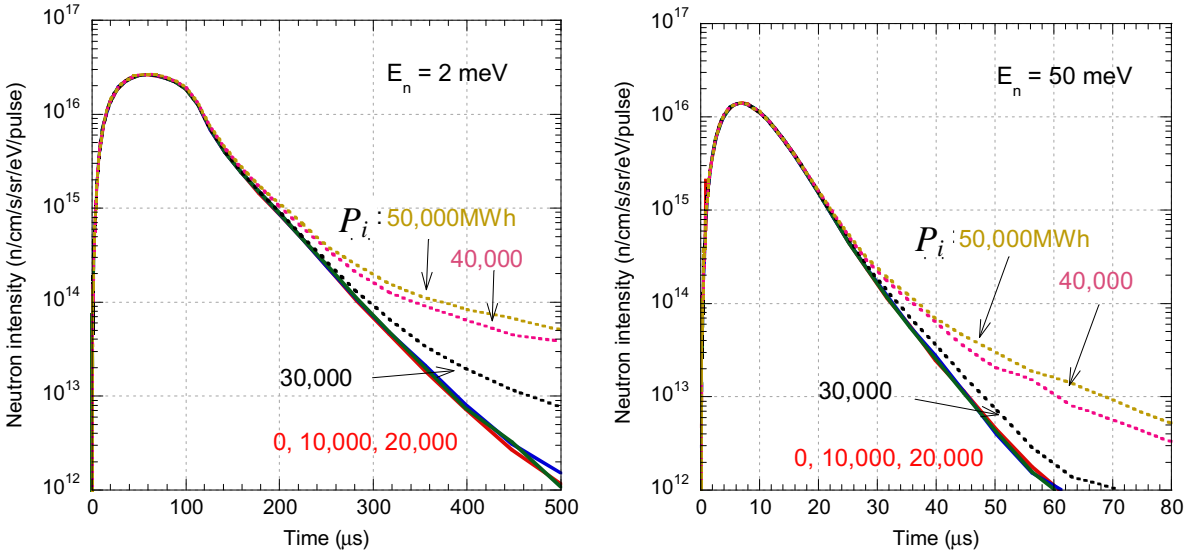

Fig. 7. Pulse shapes of AuIC decoupler at E_n = 2 and 50 meV as a function of P_i.

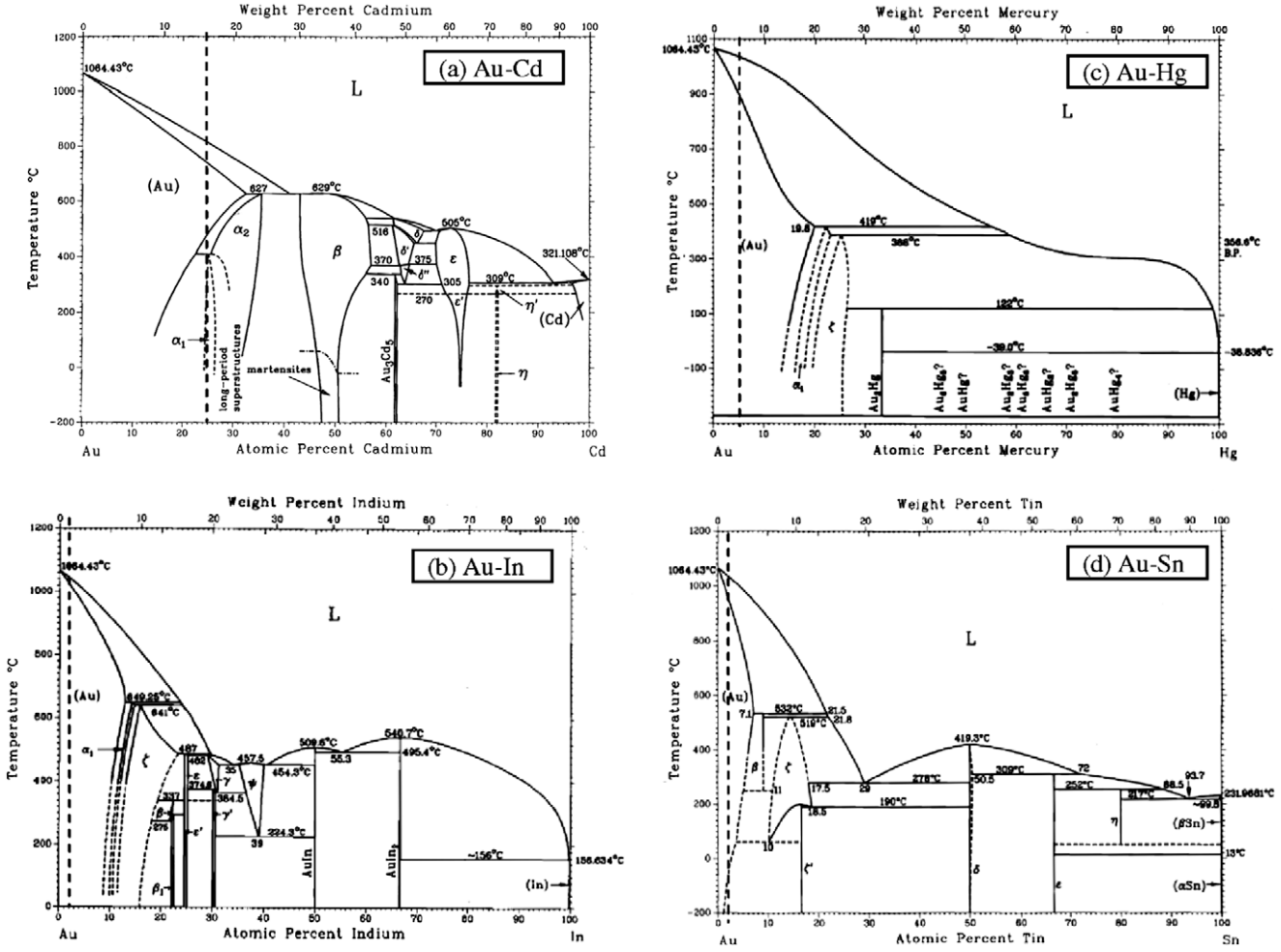

Fig. 8. Phase diagram of (a) Au–Cd, (b) Au–In, (c) Au–Hg and (d) Au–Sn system from the Ref. [9]. A vertical broken line in each figure implies the composition of the AuIC decoupler at P_i = 30,000 MWh.

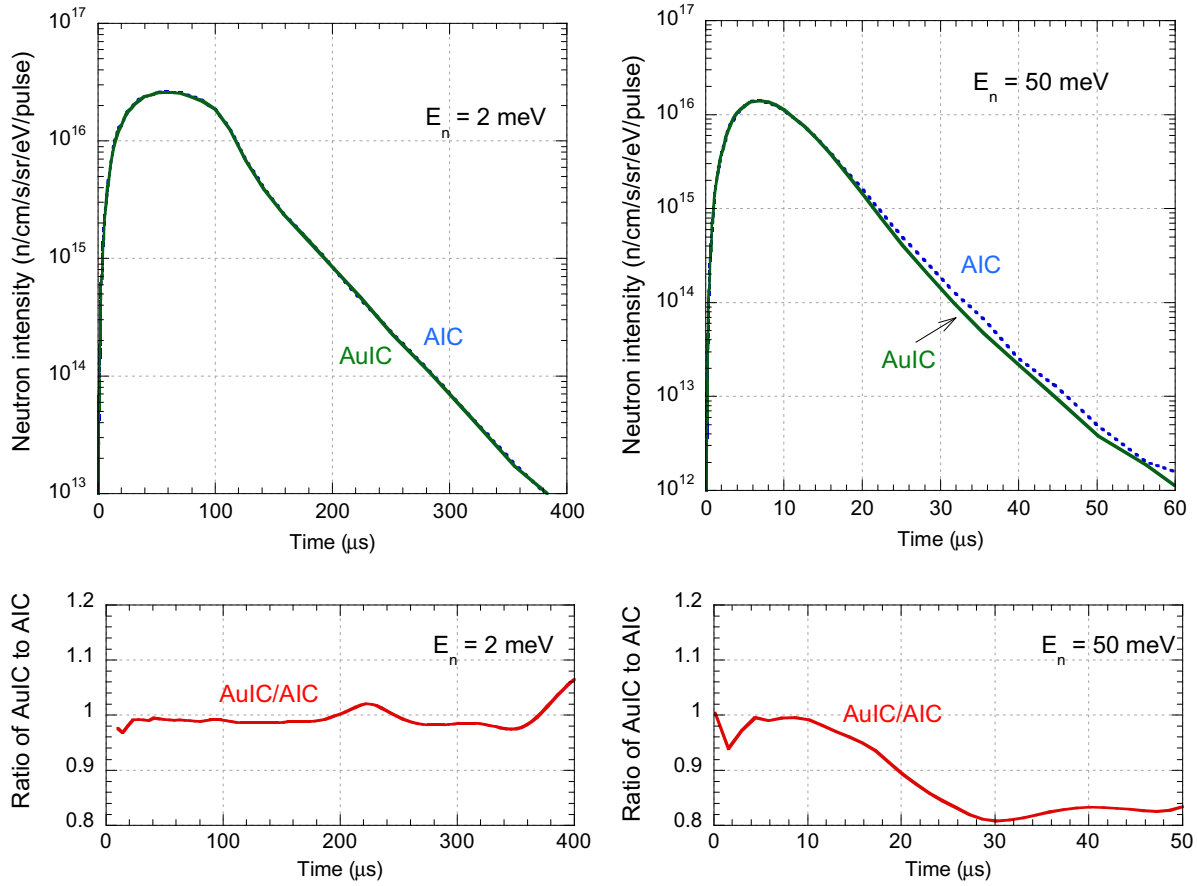

Fig. 9. Comparison of pulse shapes (upper) in case of the AuIC decoupler with those in case of the AIC decoupler at E_n = 2 (left) and 50 meV (right). Lower figures show ratio of the AuIC decoupler case to the AIC decoupler case in upper figures to make it easy to compare.

P_i = 30,000 MWh. In the all systems, phases stay in the Au-solved region throughout their life time. Therefore, we think that swelling will be negligibly small since no phase transition occurs during the irradiation. No significant problem in the AuIC decoupler is expected like the AIC decoupler.

3.2. Pulse characteristics

Fig. 9 compares pulse shapes for the AuIC decoupler with those for the AIC decoupler at E_n = 2 and 50 meV. The composition of the AIC decoupler is taken from Ref. [3]. Pulse shapes of the AuIC decoupler at the peak and the tail are almost the same as those of the AIC decoupler at both E_n. Fig. 10 shows comparison of time-integrated intensity (I_{int}), pulse width in full width at half maximum (FWHM) and pulse width in full width at 1/100 maximum ($\Delta t_{1/100}$) for the AuIC decoupler with those for the AIC decoupler. This result clearly indicates that pulse characteristics of the AuIC decoupler are almost the same as those of the AIC decoupler. $\Delta t_{1/100}$ of the AuIC decoupler at higher E_n, (10 meV–1 eV) is improved compared with that of the AIC decoupler. The reason is that the Au as neutron absorber is effective (see the AuIC transmission curve among resonance peaks in Fig. 3).

3.3. Radioactivity of AuIC decoupler

Fig. 11 shows residual radioactivity in the AuIC decoupler compared with that in the AIC decoupler at P_i = 30,000 MWh. In this figure, vertical axis is not radioactivity in Bq but converted to dose rate with assuming a point source in order to directly indicate effects to workers. Though ^{198}Au ($T_{1/2}$: 2.8 days) in the AuIC decoupler case is the largest residual radioactivity at the beginning, dose rate for the AuIC decoupler decreases by three orders of magnitude after 1 month cooling. The dose rate for the AuIC decoupler at 3 years cooling is about 100,000 times lower than that at the start of cooling. At that time, major residual radioactive isotope is ^{101}Rh ($T_{1/2}$: 3.3 years). On the other hand, major residual radioactive isotope in the AIC decoupler is ^{110m}Ag ($T_{1/2}$: 250 days) in the period from the start of cooling to 2 years. After 2 years cooling, ^{108m}Ag ($T_{1/2}$: 418 years) remains for a long time. Accordingly, the residual radioactivity in the AuIC decoupler after 5 years cooling when the moderator is handled in the facility is about two orders of magnitude lower than that in the AIC decoupler. After 30 years cooling, the difference get more clear as three orders of magnitude that enable us much easier handling and storage for final disposal of the moderators.

Total decay heat of the AuIC decoupler and the AIC decoupler at P_i = 30,000 MWh during the operation are 7.3 and 6.5 kW, respectively. After the shutdown, although that of the AIC decoupler quickly decreases, that of the AuIC decoupler slowly decreases according to the decay of ^{198}Au ($T_{1/2}$: 2.8 days). At 1 year cooling, although that of the AIC decoupler is 140 W, that of the AuIC decoupler is about 1 W.

4. Conclusions

As a result of the detailed burn-up calculation, the initial composition of the AuIC decoupler without significant pulse deterioration till the assumed life time of 30,000 MWh was determined. It was demonstrated that the AuIC decoupler could provide excellent neutron pulses with high E_d as same as the AIC decoupler. As a re-

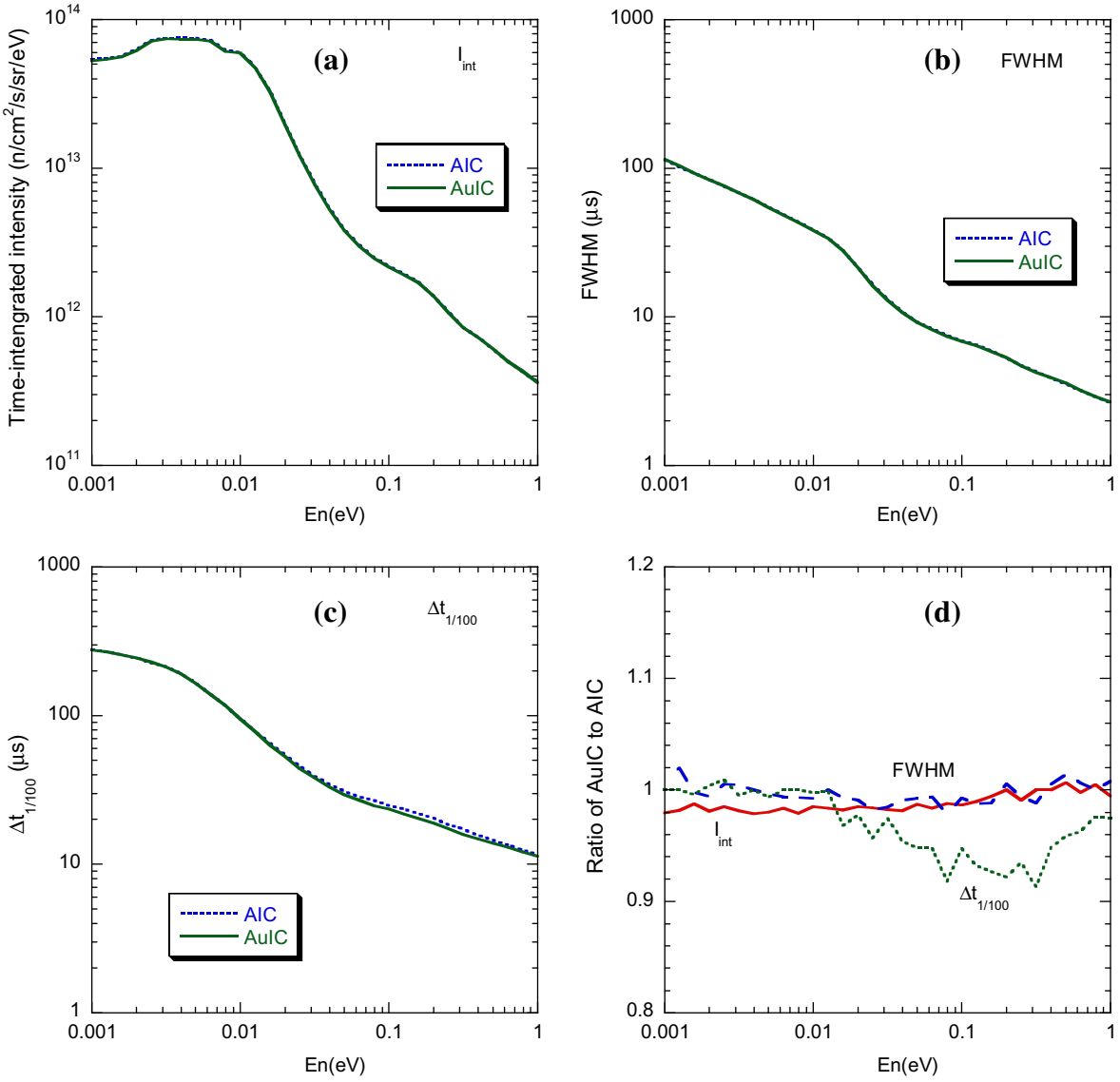

Fig. 10. Comparison of I_{int} (a), FWHM (b) and $\Delta t_{1/100}$ (c) in the AuIC decoupler case (line) with those in the AIC decoupler case (broken line). (d) shows ratio of I_{int}, FWHM and $\Delta t_{1/100}$ in the AuIC decoupler to those in the AIC decoupler to make it easy to compare.

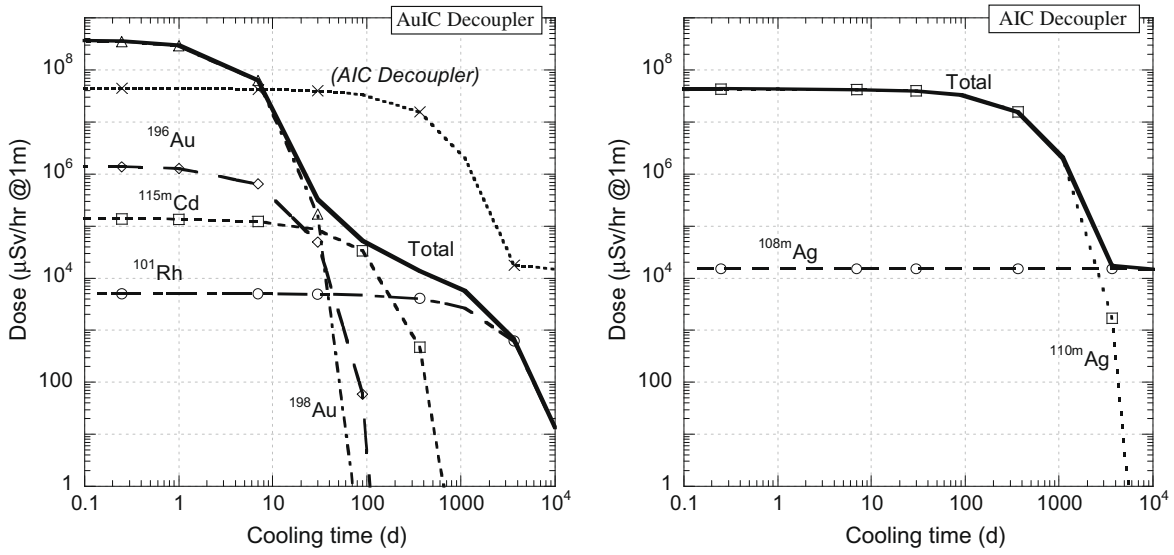

Fig. 11. Residual radioactivity of AuIC decoupler (left figure) and AIC decoupler (right figure). These values are converted to the dose rate. Dotted line in the left figure shows the residual radioactivity of the AIC decoupler shown in right figure to compare.

sult of the residual radioactivity calculation, the residual radioactivity in the AuIC decoupler was much smaller than that in the AIC decoupler at long cooling time. This meant that the use of the AuIC decoupler made the handling and storage of the moderators much easier.

As the next step, to realize the AuIC decoupler, we will study the AuIC alloy on a viewpoint of manufacturing. At early time, we will make samples of the AuIC alloy to study material property. In addition, we will also do neutron irradiation experiments of the AuIC in order to store irradiation data.

If the AuIC decoupler is realized, it is supposed that, as other applications, the AuIC can be used as control rods in a nuclear reactor.

Acknowledgements

The authors would like to acknowledge staffs of Center for Promotion of Computational Science and Engineering in JAEA for providing a parallel computer system, called PC Cluster for an exclusive use of the present calculations.

References

[1] M. Harada et al., in: Proceedings of the 16th Meeting of the International Collaboration on Advanced Neutron Sources (ICANS-XVI), Düsseldorf-Neuss, Germany, May 12–15, vol. 2, ISSN 1433-559X, ESS 03-136-M1, Forshungszentrum Jülich, 2003, p. 677.
[2] M. Teshigawara et al., J. Nucl. Mater. 343 (2005) 154.
[3] M. Teshigawara et al., J. Nucl. Mater. 356 (2006) 300.
[4] H. Iwase, K. Niita, T. Nakamura, J. Nucl. Sci. Technol. 39 (2002) 1142.
[5] J.F. Briesmeister (Ed.), MCNP™ – A General Monte Carlo N-Particle Transport Code, Version 4C, LA-13709-M, Los Alamos National Laboratory, 2000.
[6] T. Nakagawa, K. Shibata, S. Chiba, J. Nucl. Sci. Technol. 32 (1995) 1259.
[7] K. Shibata et al., J. Nucl. Sci. Technol. 34 (1997) 1171.
[8] T. Kai et al., DCHAIN-SP 2001: High Energy Particle Induced Radioactivity Calculation Code, JAERI-Data/Code 2001-016, Japan Atomic Energy Research Institute, 2001 (in Japanese).
[9] T.B. Massalski et al. (Eds.), Binary Alloy Phase Diagrams, ASM International, 1990.